Bull. Astr. Soc. India (1996) **24**, 161–170

Using Solar Oscillations to Constrain the Equation of State and Low-Temperature Opacities

J. A. Guzik, A. N. Cox, and F. J. Swenson

Los Alamos National Laboratory, Los Alamos, NM 87545 USA

Abstract. Because thousands of solar p-mode oscillation frequencies have been measured to high accuracy, direct comparisons between calculated and observed frequencies are an excellent means of testing solar interior physics. Here we compare observed and calculated nonadiabatic frequencies of solar models that include diffusive settling of helium and heavier elements. We consider the effects of low-temperature opacities, equation of state, and a nonequilibrium radiation diffusion treatment on solar structure and oscillations.

Key words: Sun: oscillations, Sun: interior, Sun: diffusion, Sun: evolution

1. Introduction

We use the forward method of directly comparing observed and calculated oscillation frequencies as a test of physics recently incorporated into our solar models. Here we compare models that use the MHD (Hummer & Mihalas 1988; Mihalas, Dappen & Hummer 1988) equation of state (EOS) tables, the Livermore OPAL (Rogers, Swenson & Iglesias 1995) EOS tables, or an analytical equation of state developed by Swenson, Irwin & Rogers (1996) that closely approximates the OPAL EOS tables, but readily accomodates variable Z mixtures. We also discuss the effects of modifications to the solar surface structure produced by low-temperature opacities and turbulent pressure on oscillation frequencies. Finally, we give preliminary results of a nonequilibrium diffusion treatment of energy transport on nonadiabatic frequency calculations.

2. Solar Models and Oscillation Frequencies

2.1 MHD EOS

Our baseline solar models use the MHD equation of state, and the OPAL (Rogers & Iglesias 1992) opacity tables, supplemented by the Alexander & Ferguson (1994) low-

temperature tables. The opacity tables were computed with the Grevesse & Noels (1993) solar element mixture. We incorporate a sinusoidally weighted average between the Alexander/Ferguson and OPAL tables between 6,500 and 9,500 K to produce a smooth transition in both opacities and opacity derivatives. Our models also include diffusive settling (gravitational, thermal, and chemical) of helium and heavier elements according to the prescription of Burgers (1969) (see Cox, Guzik & Kidman 1989). We interpolate in both Y and Z in the opacity tables, thereby accounting for the effects of element diffusion on opacities. The MHD EOS tables are computed for Z=0.02, so we take into account the effects of helium diffusion, but not Z diffusion on the EOS.

The solar evolution and nonadiabatic pulsation frequency calculations are described in Cox, Guzik & Kidman (1989), and Guzik & Cox (1995). We use the Iben (1963, 1965) evolution code, vary the initial helium abundance and constant mixing length/pressure scale height ratio α to match the solar luminosity 3.846 x 10^{33} erg/sec and radius 6.9599 x 10^{10} cm at the present solar age 4.54 $\pm$ 0.04 Gyr (Guenther 1989). Nuclear reaction rates are from Caughlan & Fowler (1988). We use the composition profile from the evolution model to produce a finely-zoned (1700 zone) model that tracks nearly exactly the structure of the evolution model for input into the linear nonradial nonadiabatic Lagrangean pulsation code of Pesnell (1990).

Figure 1 shows the observed minus calculated (O-C) nonadiabatic frequencies as a function of calculated frequency for the low-degree modes ($\ell = 0, 1, 2, 3$) for a model with initial (Y, Z) abundance (0.276, 0.0195), and $\alpha = 1.72$. Lines connect modes of the same degree ℓ and different radial order n. The convection zone base for this model is at about 0.715 $R_\odot$, slightly shallower than the convection zone depth inferred from the sound speed discontinuity seen in helioseismic inversions 0.713 $\pm$ 0.003 $R_\odot$ (Christensen-Dalsgaard et al. 1991). For this model, the calculations agree with observations to within a few microhertz. There is a systematic decrease in O-C frequency with increasing frequency up to $\sim$ 3600 μHz. Also, there is an increase in O-C for $\nu > 3600$ μHz, because the diffusion approximation of radiation transport that we use in the frequency calculations overestimates the nonadiabatic corrections. Figure 2 shows the intermediate-degree O-C frequencies for this model, and Fig. 3 shows the high-degree modes. The agreement with observation becomes poorer for increasing degree ℓ, indicating a significant difference between the model structure and the actual solar structure near the surface.

2.2 Effects of surface physics variations on frequencies

There are many suggested modifications to the physics of modeling the Sun's surface layers that can improve the agreement between our predicted frequencies and observations. Among these are modifying the low-temperature opacities, including turbulent pressure, and using more sophisticated convection treatments. Alternatives to the mixing length treatment of convection and their effect on solar structure and oscillations are discussed by Paterno et al. (1993), and Rosenthal et al. (1995).

a. Low temperature opacities and turbulent pressure

Neuforge (1993) compared available low-temperature opacity tables, and found that there are significant differences (up to a factor of two) between them, even when the same opacity contributors are reportedly included in the calculations. The close agreement between

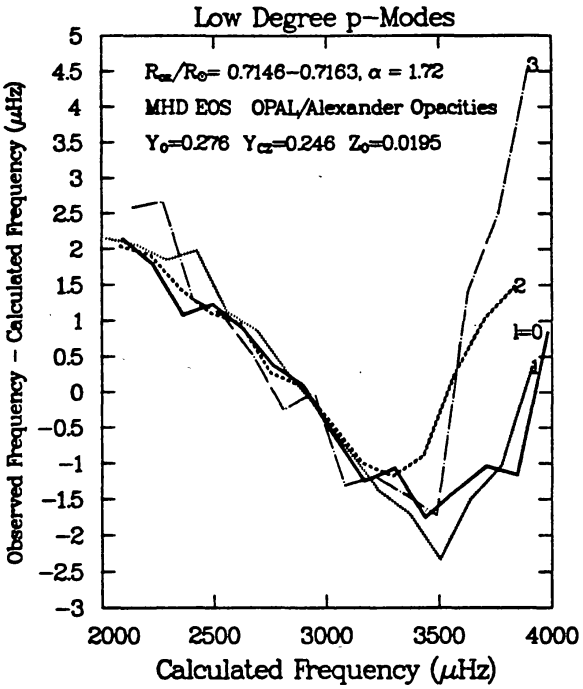

Figure 1. Observed minus calculated (O-C) vs. calculated p-mode frequencies of degree $\ell = 0, 1, 2,$ and 3 for solar model including diffusive settling of helium and heavier elements, MHD EOS, OPAL opacities, and Alexander/Ferguson low-temperature opacities. Lines connect modes of same degree ℓ and different radial order n. Observations are from Anguera Gubau et al. (1992).

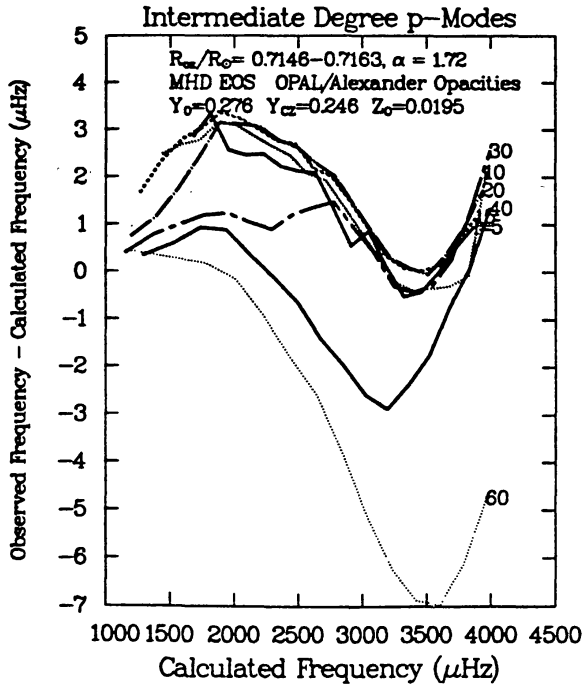

Figure 2. O-C vs. calculated p-mode frequencies of degree $\ell = 5, 10, 15, 20, 30, 40,$ and 60 for MHD EOS solar model described in Fig. 1. Lines connect modes of same degree ℓ and different radial order n. Observations are from Libbrecht et al. (1990).

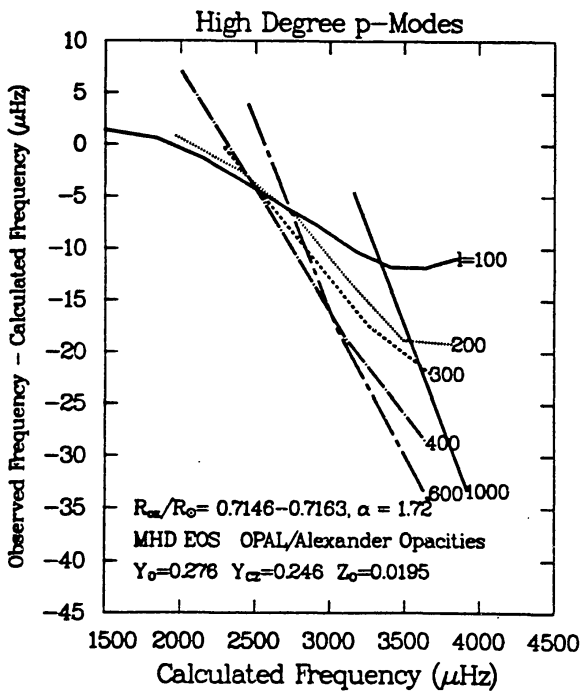

Figure 3. O-C vs. calculated p-mode frequencies of degree $\ell = 100, 200, 300, 400, 600$, and 1000 for MHD EOS solar model described in Fig. 1. Lines connect modes of same degree ℓ and different radial order n. Observations are from Libbrecht et al. (1990).

recent tables of Kurucz (1992) and Alexander/Ferguson (G. Houdek 1995, private communication), might lead one to believe that researchers are converging on agreed-upon Rosseland mean opacities. Nevertheless, if we could determine with confidence the effects of other uncertainties in modeling solar surface structure, it would be possible to use solar oscillations to constrain low-temperature opacities.

For example, we evolved a solar model with opacities increased by 50% for $T < 15,000$ K. Figure 4 compares the temperature versus density profile near the surface of our solar models with and without this opacity increase. The enhanced-opacity model requires a larger α (2.12 instead of 1.72) to match the solar radius due to this change in the superadiabatic temperature gradient near the top of the convection zone. In the enhanced-opacity model, we also increased the initial Z slightly (to 0.0205) to deepen the convection zone. We have found that adjusting the convection zone base radius vertically shifts the O-C frequencies for modes with turning points below the convection zone (Guzik & Cox 1993). However, the small change in initial Z does not affect the systematic decrease in O-C with increasing frequency seen in Fig. 1.

The solar surface structure modification (due to the increased low-temperature opacities) does improve the O-C decrease with increasing frequency for $\nu < 3600$ μHz, as seen in Fig. 5. Figure 6 shows that the high-degree frequencies ($\ell = 100 - 1000$) also agree better with observations (compare with Fig. 3), but the general decrease in O-C with increasing frequency persists. Figure 7 shows that including frequency corrections due to turbulent pressure (as calculated by Guzik & Cox 1992), in addition to the surface opacity increase, further improves the agreement with observations for the high-degree modes. However, Rosenthal et al. (1995) note that including not only turbulent pressure,

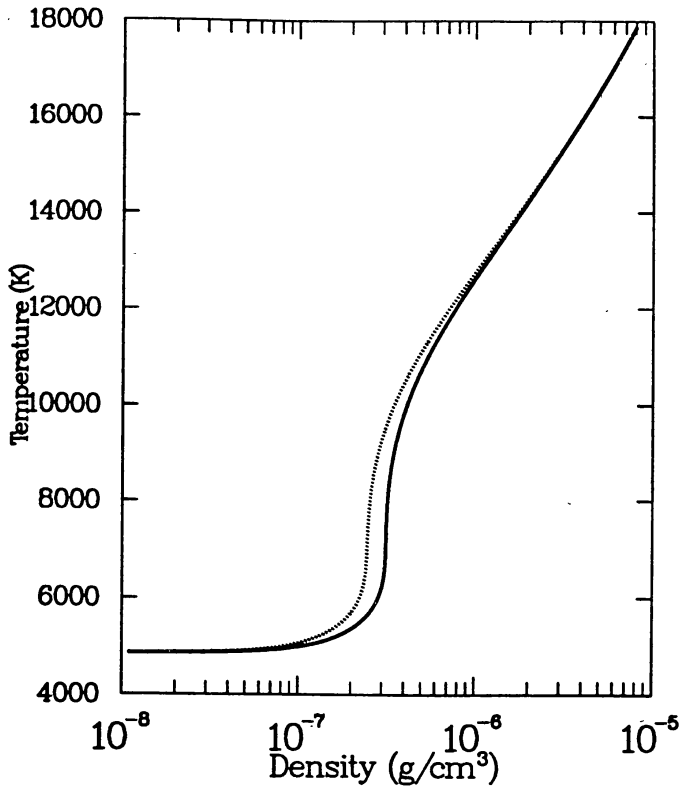

Figure 4. Temperature vs. density profile near the surface of solar models using the MHD EOS, with (dotted line) and without (solid line) a 50% opacity increase for temperatures < 15,000 K.

but also the fluctuations in turbulent pressure via a time-dependent mixing length theory of convection, may reduce the frequency corrections produced by turbulent pressure.

b. Nonequilibrium radiation diffusion

In our calculations, nonadiabatic effects decrease the frequencies by up to about 6 μHz for $\nu < 3600$ μHz. We use the radiation diffusion approximation in our pulsation calculations, even in the optically thin regions. This overestimates the nonadiabatic corrections at high frequencies, and causes the steep rise in O-C for $\nu > 3600$ μHz seen in Fig. 1. Guenther (1994) finds that adding a term including the time derivative of the entropy S to the mean radiation intensity J removes most of this systematic error. However, in this approximation S is the total entropy, when it should be the matter entropy. To be consistent, a bi-system oscillation theory should be implemented (Li 1992), in which J does not equal the Planck function B. This formulation allows the matter and radiation temperatures, their entropies, and their fluctuations, to vary independently of one another. We implemented this nonequilibrium diffusion treatment in the Pesnell pulsation code. Our preliminary results show that, at least for the low-degree modes, the nonadiabatic frequencies are increased somewhat with increasing frequency, and the systematic errors caused by the diffusion approximation are removed. For example, the correction to the nonadiabatic frequencies is +2.3 μHz at $\sim 3200\mu$Hz, and +8.9 μHz at $\sim 4000\mu$Hz.

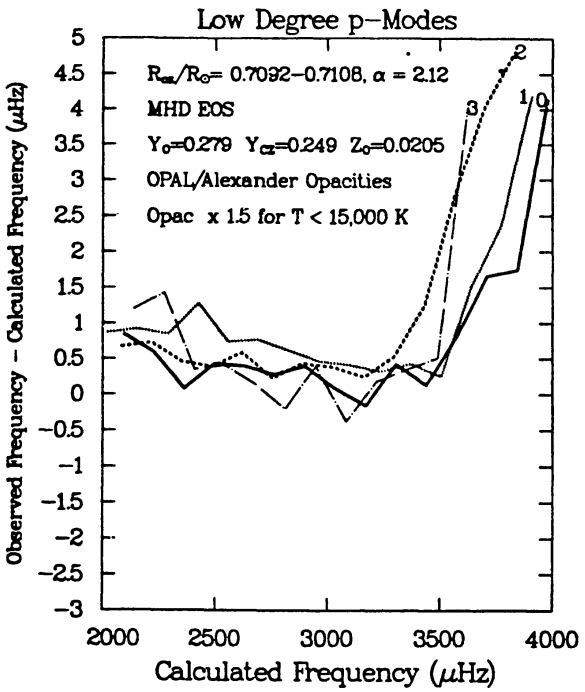

Figure 5. O-C vs. calculated p-mode frequencies of degree $\ell = 0, 1, 2$, and 3 for MHD EOS model with 50% opacity increase for temperatures $< 15,000$ K. The change in model structure produced by this opacity increase (Fig. 4) removes the systematic decrease in O-C frequency with increasing frequency for $\nu < 3600\mu$Hz.

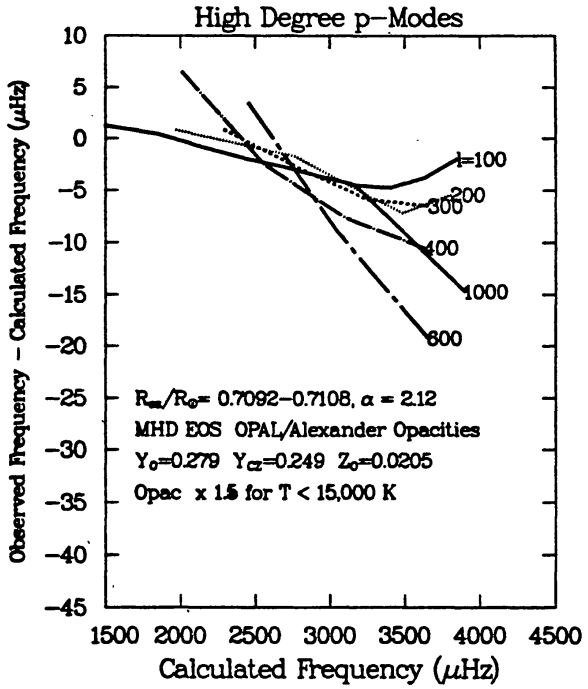

Figure 6. O-C vs. calculated p-mode frequencies of degree $\ell = 100, 200, 300, 400, 600$, and 1000 for MHD EOS model with 50% opacity increase for temperatures $< 15,000$ K. The opacity increase improves the agreement with observation for these high-degree modes (compare with Fig. 3).

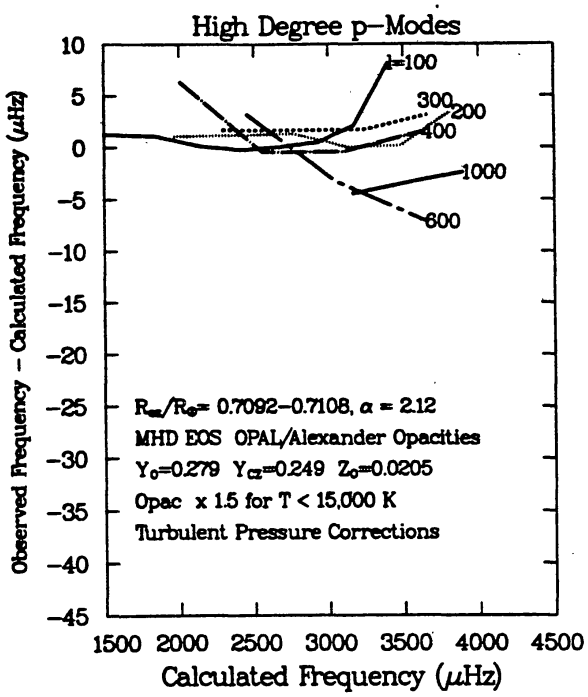

Figure 7. O-C vs. calculated p-mode frequencies of degree ℓ = 100, 200, 300, 400, 600, and 1000 for MHD EOS model with 50% opacity increase for temperatures < 15,000 K, and including frequency corrections due to turbulent pressure as calculated by Guzik & Cox (1992). Turbulent pressure further improves agreement with observation for these high-degree modes.

2.3 Livermore OPAL EOS tables and Swenson et al. analytical EOS

Here we compare observed and calculated frequencies of solar models using the OPAL (Rogers, Swenson & Iglesias 1995) EOS tables and an analytical EOS of Swenson, Irwin & Rogers (1996; see also Swenson 1995) that closely approximates the OPAL EOS tables. The Swenson et al. analytical EOS can readily account for variations in Z and in the element mixture. This feature makes the Swenson et al. EOS extremely useful for studying the effects of element diffusion, or using oscillations to constrain abundances.

The EOS computation approach used by OPAL is entirely different from that used by MHD. MHD is formulated in the chemical picture using the free-energy minimization method, whereas OPAL uses a physical picture, in which the grand canonical partition function is expanded in terms of fundamental constitutents (electrons and nuclei). For further details, see the article by W. Dappen (these proceedings).

Figure 8 shows the O-C versus calculated low-degree nonadiabatic frequencies for the model using the OPAL EOS tables computed for Z=0.02, as in our MHD model, but for a somewhat different element mixture. This model includes helium and element diffusion, interpolates in Y and Z in the opacity tables, but does *not* include the low-temperature opacity increase. For the same initial Z abundance (0.0195) as our comparison MHD model, the OPAL EOS model has a slightly deeper convection zone than the MHD model. The model also requires a lower initial Y abundance (0.274 instead of 0.276) to produce the present solar luminosity, because the OPAL EOS tables include electron exchange terms that slightly decrease the central pressure. The electron exchange terms are not included in either the MHD EOS, or the Swenson analytical EOS used here.

Figure 9 shows the high-degree ($\ell = 100-1000$) frequencies for the OPAL EOS model. The agreement between calculated and observed high-degree frequencies is somewhat improved compared to the O-C frequencies of the MHD model (Fig. 3). This is probably attributable to a substantial pressure difference (about 1.2%) between the OPAL and MHD EOS at about 50,000 K (in the helium ionization zone); the MHD EOS pressure is too high due to application of the "tau(x)" correction outside its region of validity (see article by Dappen, these proceedings; and Graboske et al. 1969).

For the Swenson et al. EOS model, we allow the Z abundance to vary in the EOS calculation according to the composition profile produced by element diffusion. Figure 10 shows that the high-degree frequencies of the Swenson et al. analytical EOS model are only slightly different from those of the model using the OPAL EOS table interpolation (compare with Fig. 9). These frequency differences might be due to small differences between the two EOS's, but more likely are due to the proper allowance for variable Z (due to diffusion) in the Swenson et al. EOS. This comparison suggests that neglect of Z diffusion in the EOS interpolation has a small, but potentially measurable effect.

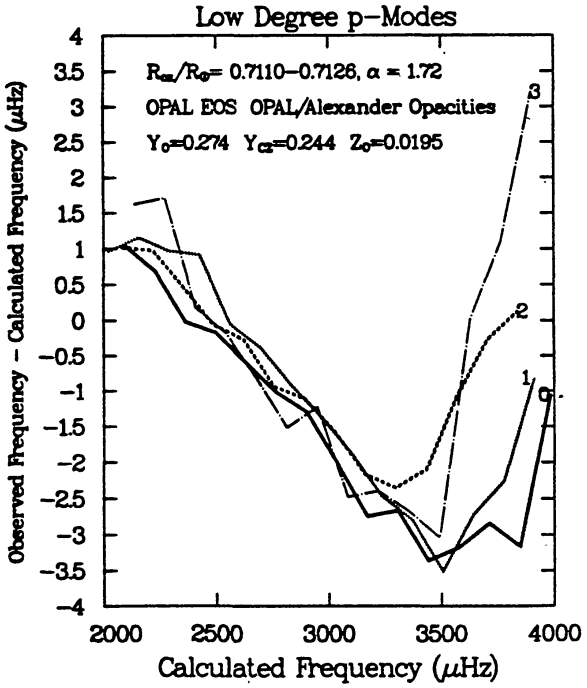

Figure 8. O-C vs. calculated p-mode frequencies of degree $\ell = 0, 1, 2$, and 3 for OPAL EOS model. Compare with Fig. 1 for the equivalent solar model with the MHD EOS. Compared to the MHD EOS nodel, the OPAL EOS model has a slightly deeper convection zone, and requires a lower initial Y to match the present solar luminosity.

3. Conclusions

The calculated nonadiabatic frequencies for a solar model including helium and element settling and the latest opacities and equation of state match observed frequencies to within about 10 μHz for degrees $\ell < 100$ and about 50 μHz for $\ell > 100$. Including a

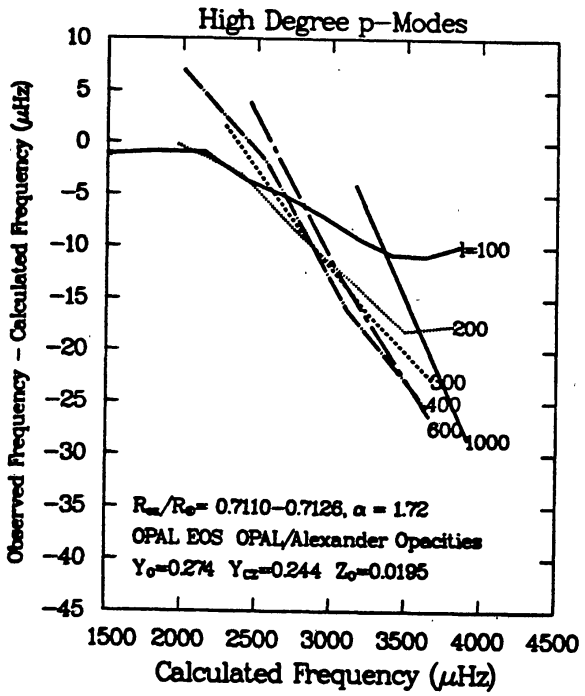

Figure 9. O-C vs. calculated p-mode frequencies of degree $\ell = 100, 200, 300, 400, 600$, and 1000 for OPAL EOS model. Compare with Fig. 3 for the MHD EOS model. The improvement with observations for the OPAL EOS model is probably due to the 1.2% lower pressure of the OPAL EOS at temperatures $\sim 50,000$ K.

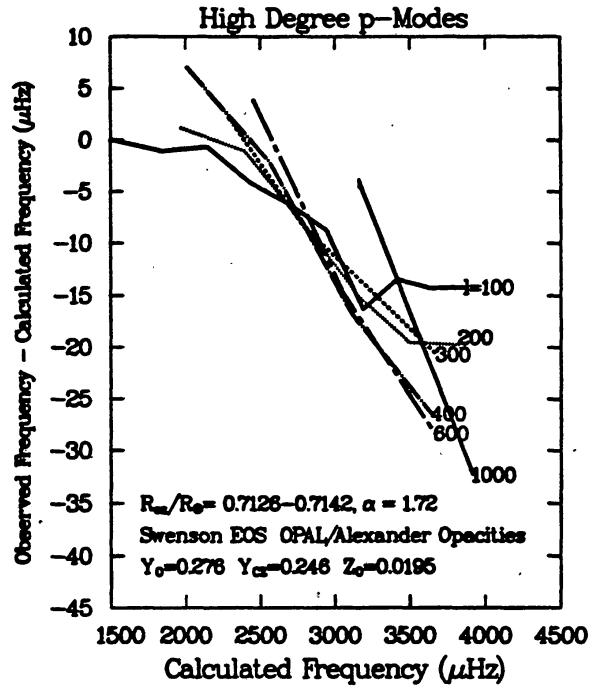

Figure 10. O-C vs. calculated p-mode frequencies of degree $\ell = 100, 200, 300, 400, 600$, and 1000 for solar model using the Swenson et al. analytical EOS that closely approximates the OPAL EOS tables. The frequencies are probably different (compare with Fig. 9) because the Swenson et al. EOS takes into account changes in the Z profile produced by element diffusion.

nonequilibrium radiative diffusion treatment removes the overestimate of nonadiabatic corrections at high frequency caused by the radiation diffusion approximation.

We can remove most of our systematic O-C decrease with increasing frequency by modifying the structure of the superadiabatic regions of the model. We accomplish this by increasing the low-temperature opacities over the Rosseland mean values of Alexander/Ferguson by $\sim 50\%$. Turbulent pressure may further decrease the remaining O-C residuals for high-degree modes. However, other improvements in modeling the solar surface structure, such as more sophisticated convection treatments, can also produce the desired frequency corrections.

Solar models using the OPAL EOS have slightly deeper convection zones, and require a slightly lower initial helium abundance to match the solar luminosity. The high-degree ($\ell = 100-1000$) frequencies of the models using the OPAL EOS tables or the Swenson et al. analytical EOS match observations better than those of the MHD EOS model. This difference is probably due to the 1.2% higher pressure of the MHD EOS near 50,000 K.

The authors thank G. Houdek, J. Christensen-Dalsgaard, M. Gabriel, A. Kosovichev, P. Bradley, D. Pesnell, F. Rogers, and D. Alexander for useful discussions.

References

Alexander D.R., Ferguson J.W., 1994, ApJ, 437, 879.
Anguera Gubau M., Palle P.L., Perez Hernandez F., Regulo C., Roca Cortes T., 1992, A&A, 255, 363.
Burgers J.M., 1969, in Flow Equations for Composite Gases, New York: Academic Press.
Caughlan G.R., Fowler W.A., 1988, Atomic Nucl. Data Tables, 40, 283.
Christensen-Dalsgaard J., Gough D.O., Thompson M.J., 1991, ApJ, 378, 413.
Cox A.N., Guzik J.A., Kidman R.B., 1989, ApJ, 342, 1187.
Graboske H.C., Harwood D.J., Rogers F.J., 1969, Phys. Rev., 186, 210.
Grevesse N., Noels A., 1993, in Origin and Evolution of the Elements, eds.S. N. Prantzos, E. Vangioni-Flam, and M. Casse, Cambridge University Press.
Guenther D.B., 1989, ApJ, 339, 1156.
Guenther D.B., 1994, ApJ, 422, 400.
Guzik J.A., Cox A.N., 1992, ApJ, 386, 729.
Guzik J.A., Cox A.N., 1993, ApJ, 411, 394.
Guzik J.A., Cox A.N., 1995, ApJ, 448, 905.
Hummer D.G., Mihalas D., 1988, ApJ, 331, 794.
Iben I., 1963, ApJ, 138, 452.
Iben I., 1965, ApJ, 141, 993.
Kurucz R.L., 1992, Rev. Mexicana Astron. Astrof., 23, 181.
Li Y., 1992, A&A, 133, 257.
Libbrecht K.G., Woodard M.F., Kaufman J.M., 1990, ApJS, 74, 1129.
Mihalas D., Dappen W., Hummer D.G., 1988, ApJ, 331, 815.
Neuforge C., 1993, A&A, 274, 818.
Paterno L., Ventura R., Canuto,V. M., Mazzitelli I., 1993, ApJ, 402, 733.
Pesnell W.D., 1990, ApJ, 363, 227.
Rogers F.J., Iglesias C.A., 1992, ApJS, 179, 507.
Rogers F.J., Swenson F.J., Iglesias C.A., 1995, ApJ, in press.
Rosenthal C.S., Christensen-Dalsgaard J., Houdek G., Monteiro M.J.P.F.G, Nordlund A., Trampedach R., 1995, "Seismology of the Solar Surface Regions", in 4th SOHO Workshop: Helioseismology, ESA SP-376, ESTEC, Noordwijk.
Swenson F.J., 1995, ApJ, 438, L87.
Swenson F.J., Rogers F.J., Irwin A., 1996, in preparation.